THE JOURNAL OF PHYSICAL CHEMISTRY A

Article

Cite This: J. Phys. Chem. A 2019, 123, 4599−4608

pubs.acs.org/JPCA

Charged Clusters of C_{60} and Au or Cu: Evidence for Stable Sizes and Specific Dissociation Channels

Paul Martini,[†] Marcelo Goulart,[†] Lorenz Kranabetter,[†] Norbert Gitzl,[†] Bilal Rasul,[†,‡] Paul Scheier,*[,†] and Olof Echt*[,†]

[†]Institut für Ionenphysik und Angewandte Physik, Universität Innsbruck, Technikerstr. 25, A-6020 Innsbruck, Austria

[‡]Department of Physics, University of Sargodha, 40100 Sargodha, Pakistan

ABSTRACT: We have doped helium nanodroplets with C_{60} and either gold or copper. Positively or negatively charged $(C_{60})_mM_n^{\pm}$ ions (M = Au or Cu) containing up to ≈10 fullerenes and ≈20 metal atoms are formed by electron ionization. The abundance distributions extracted from high-resolution mass spectra reveal several local anomalies. The sizes of the four most stable $(C_{60})_mAu_n^{\pm}$ ions identified in previous calculations for small values of m and n ($m \leq 2$ and $n \leq 2$, or $m = 1$ and $n = 3$) agree with local maxima in the abundance distributions. Our data suggest the existence of several other relatively stable ions including $(C_{60})_2Au_3^{\pm}$ and $(C_{60})_3Au_4^{-}$. Another feature, namely the absence of bare $(C_{60})_2^{\pm}$, confirms the prediction that $(C_{60})_2M^{\pm}$ dissociates by loss of $C_{60}^{\pm}$ rather than loss of M. The experimental data also reveal the preference for loss of (charged or neutral) C_{60} over loss of a metal atom from some larger species such as $(C_{60})_3M_3^{+}$. In contrast to these similarities between Au and Cu, the abundance distributions of $(C_{60})_3Au_n^{-}$ and $(C_{60})_3Cu_n^{-}$ are markedly different. In this discussion, we emphasize the similarities and differences between anions and cations, and between gold and copper. Also noteworthy is the observation of dianions $(C_{60})_mAu_n^{2-}$ for m = 2, 4, and 6.

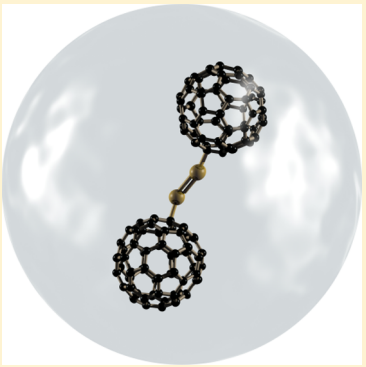

1. INTRODUCTION

Interest in fullerene−metal complexes has a long history. The possibility to cage lanthanum atoms in C_{60} was already envisioned in the seminal paper by Kroto et al. in *Nature*.[1] Six years later, superconductivity of fullerene films intercalated with alkali atoms was discovered.[2] Fullerenes coated with alkali, alkaline earth, or other metals are candidates for high-density hydrogen storage.[3−6] Compounds of fullerenes with transition metals have various potential applications as nanomaterials,[7] including their role in ternary bulk heterojunction organic photovoltaic cells.[8]

Several groups have studied the interaction between C_{60} and coinage metals by vapor deposition on films; most of these studies pertain to gold. Kröger et al. have deposited C_{60} on gold films as well as Au on C_{60} films; X-ray photoelectron spectroscopy (XPS) and ultraviolet photoelectron spectroscopy (UPS) indicated that the interaction between Au and C_{60} is covalent but lacks the signature of charge transfer.[9] Liu and Gao have synthesized three-dimensional fullerene−gold networks by wet chemistry in which Au nanoparticles are coated by C_{60}; Raman spectra suggested electron transfer from gold to C_{60}.[10] Conversely, Ren et al. have encapsulated clusters of C_{60} in gold.[11] Xie et al. have trapped C_{60} at the edges of two-dimensional gold islands; the smallest entities identified by scanning tunneling microscopy consisted of Au_{19} surrounded by six C_{60}.[12] In later work, it was shown that $(C_{60})_7Au_{19}$ is a magic number cluster in which six C_{60} are attached to the six-step edges of the gold island, whereas the seventh C_{60} sits directly above the island.[13]

Xiao and Zhang have prepared copper clusters coated with C_{60} by pulsed laser ablation at the interface between a copper target and a flowing fullerene solution of hexane.[14] Singhal et al. have synthesized copper clusters embedded in a C_{60} matrix by codeposition from the vapor phase, followed by irradiation of the film with energetic (120 MeV) Au^+ ions.[15] The high cohesive energy of coinage metals favors aggregation of metal atoms separated from the C_{60} phase, but codeposition of C_{60} and silver (whose cohesive energy is below that of copper and gold) at 23 K has yielded metallic Ag-intercalated C_{60} (Ag_7C_{60}) crystallites dispersed in an insulating C_{60} phase.[16]

Very few studies pertain to small, isolated complexes of C_{60} and coinage metals. Palpant et al. have prepared C_{60}−Au clusters by laser vaporization; $C_{60}Au_n^{-}$ anions with $n \leq 6$ were characterized by UPS.[17] The vertical and adiabatic detachment energies exhibited a strong odd−even effect; odd-numbered species were significantly more stable than even-numbered ones. Lyon and Andrews have recorded infrared spectra of C_{60} embedded in an argon matrix, codoped with Cu, Ag, or Au.[18] The authors concluded that the perturbation of vibrational modes increases in the order Au → Cu → Ag and that the C_{60}−Au complex has a charge transfer of about $0.5e^{-}$. Theoretical studies of the interaction between (neutral or charged) fullerenes and coinage metals have been either limited to a single metal atom[19,20] or to C_{60} sandwiched

Received: March 24, 2019
Revised: April 29, 2019
Published: May 7, 2019

DOI: 10.1021/acs.jpca.9b02768
J. Phys. Chem. A 2019, 123, 4599−4608

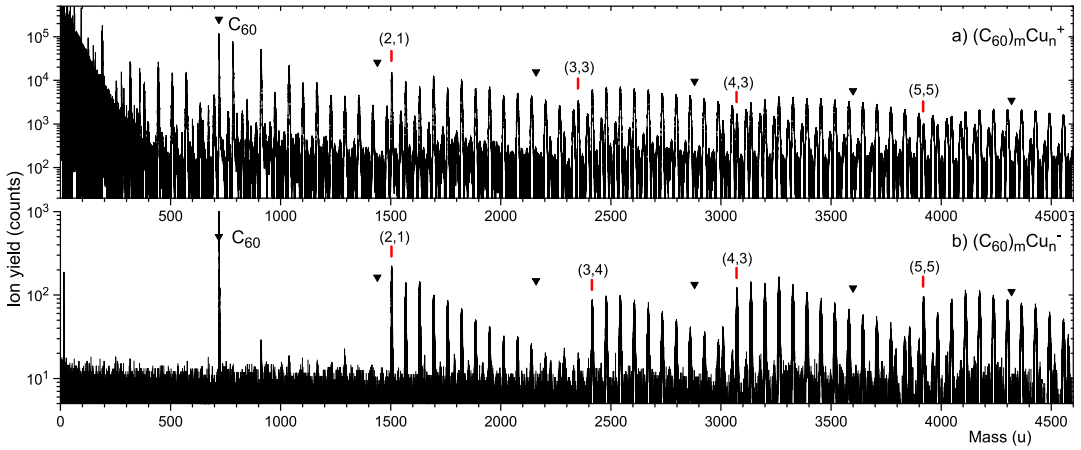

Figure 1. Mass spectra of positively and negatively charged ions (panels a and b, respectively) obtained by electron ionization of HNDs doped with C_{60} and copper. The expected positions of bare, isotopically pure $(^{12}C_{60})_m^{\pm}$ ion peaks is marked by triangles; they are virtually absent for $m > 1$. The approximate onset of each $(C_{60})_mCu_n^{\pm}$ homologous ion series (m = const) is indicated by its values of (m, n).

between two small, identical clusters of silver or gold.[20−23] A first-principle calculation of C_{60} covered with up to 92 gold atoms concludes that the fullerene−gold interaction is of the van der Waals type,[24] in conflict with later theoretical studies of smaller complexes.[20,21,25]

In a recent letter, we reported experiments in which C_{60}−gold complexes were grown inside cold (0.37 K), superfluid helium nanodroplets (HNDs) by passing the HNDs through pickup cells containing C_{60} and Au vapor at low density; the doped droplets were then ionized by electrons.[25] Positive and negative ions with the stoichiometry $(C_{60})_mAu_n^{\pm}$ where m, n are small integers were detected. One interesting observation was the relatively large abundance of $(C_{60})_2Au^{\pm}$ which suggests that this ion has enhanced stability. Density functional theory (DFT) calculations confirmed the conclusion; they predict that the two C_{60} molecules are located on opposite sides of the Au atom in a dumbbell-like arrangement.

The present contribution presents a full account of our experimental data for C_{60}−gold complexes. Furthermore, gold is rather special among coinage metals; its ability to undergo covalent bonding derives from relativistic effects which lower the energy of the 6s orbital while destabilizing the 5d orbital.[26] As a result, the character of bonding in complexes such as $M(CN)_2^-$ changes from ionic for M = Cu to strongly covalent for M = Au.[27] Previous experiments with alkali, alkaline earth, or transition metals bound to C_{60} have shown that differences in bonding character profoundly affect the stability pattern of $(C_{60})_mM_n^{\pm}$ cluster ions as revealed by mass spectrometry.[28,29] In the present contribution, we report the stability patterns of charged C_{60}−gold and C_{60}−copper complexes. The effect of the coinage metal and the charge state of the clusters (+e or −e) will be discussed. Furthermore, a series of mass peaks located midway between those due to $(C_{60})_mAu_n^-$ anions are assigned to $(C_{60})_mAu_n^{2-}$ dianions with m = 2, 4, and 6, n odd.

2. EXPERIMENTAL SECTION

HNDs were produced by expanding helium (Linde, purity 99.9999%) at a stagnation pressure of about 23−25 bar through a 5 μm nozzle, cooled by a closed-cycle cryostat (Sumitomo Heavy Industries LTD, model RDK-415D), in vacuum. Nozzle temperatures ranged from 9.2 to 9.7 K. Droplets formed at these conditions contain an average of about 5×10^5 to 10^6 atoms.[30] The resulting supersonic beam was skimmed by a 0.8 mm conical skimmer, located 8 mm downstream from the nozzle and passed through a 20 cm-long pickup region in which C_{60} was vaporized at about 650 or 580 K for experiments with copper and gold, respectively. The droplets then passed through another pickup cell filled with copper or gold vapor produced in a resistively heated oven. The temperature of the metal oven could not be measured directly; it was adjusted in order to obtain optimal conditions for the formation of mixed fullerene−metal cluster ions.

The doped HNDs passed through a differentially pumped vacuum chamber where they were crossed with an electron beam of variable energy. Anions were formed at 22 eV, whereas cations were formed at about 70 eV; the emission current ranged from 120 to 285 μA. Ions were accelerated into the extraction region of a commercial orthogonal time-of-flight mass spectrometer equipped with a reflectron (Tofwerk AG, model HTOF). The mass resolution was $m/\Delta m$ = 3000 (Δm = full width at half-maximum). The ions were detected by a microchannel plate operated in single-ion counting mode and recorded via a time-to-digital converter. Additional experimental details have been described elsewhere.[31]

Mass spectra were evaluated by means of a custom-designed software.[32] The routine takes into account the isotope pattern of all ions that might contribute to a specific mass peak by fitting a simulated spectrum with defined contributions from specific atoms to the measured spectrum in order to retrieve the abundances of specific clusters. The natural abundance of ^{13}C is only 1.07%, but the large number of carbon atoms in $(C_{60})_m$ leads to a multitude of mass peaks for each specific cluster size (for an illustration, see refs[32,33]). Gold is monoisotopic (^{197}Au), but the presence of two copper isotopes (^{63}Cu and ^{65}Cu, natural abundance 69.17 and 30.83%, respectively) makes the analysis of $(C_{60})_mCu_n$ complexes even more challenging. Furthermore, the software corrects for experimental artifacts such as background signal levels, the mass shift of the mass spectra, non-Gaussian peak shapes, and mass drift over time.

3. RESULTS

A positive ion mass spectrum of HNDs doped with C_{60} and copper is displayed in Figure 1a. Pure He_n^+ cluster ions form a prominent series below approximately 600 u, but the strongest peaks in this region are clusters of pure copper (isotopes ^{63}Cu

DOI: 10.1021/acs.jpca.9b02768
J. Phys. Chem. A 2019, 123, 4599−4608

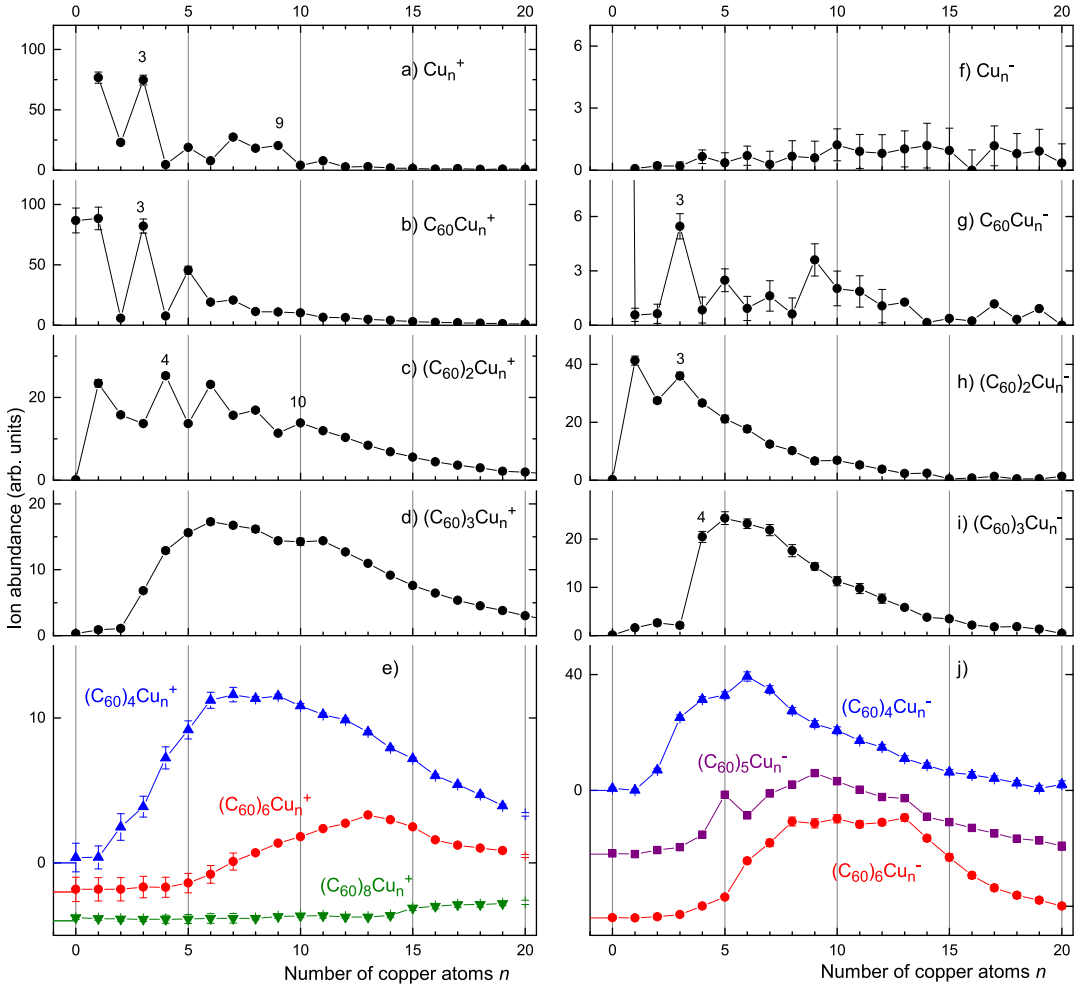

Figure 2. Abundance distributions of $(C_{60})_mCu_n^{\pm}$ $(0 \le m \le 3)$ cations and anions (left and right panels, respectively). Representative distributions for larger values of m in the bottom panels e and j are stacked; base lines are indicated by horizontal lines below $n = 0$.

and ^{65}Cu, average atomic mass 63.55 u). Homologous $(C_{60})_mCu_n^+$ ion series are prominent above 720 u, the mass of $^{12}C_{60}^+$. The expected positions of mass peaks due to $(C_{60})_m^+$ are marked by triangles; these ions are conspicuously absent for $m \ge 2$. The $(C_{60})_2Cu_n^+$ series commences at $n = 1$ while the $(C_{60})_3Cu_n^+$ ion series is barely visible below $n = 3$. $(C_{60})_4Cu_n^+$ and $(C_{60})_5Cu_n^+$ remain weak below $n = 3$ and 5, respectively. These onsets are indicated in Figure 1a by their (m, n) values, although their exact values are, admittedly, a matter of judgment.

A negative ion mass spectrum of HNDs doped with C_{60} and copper is displayed in Figure 1b. Experimental parameters used to generate and dope the HNDs were similar to those used for the positive ion spectrum (see Section 2 for details). By and large, the spectrum of anions resembles that of cations above the mass of the fullerene dimer. However, the yield of $(C_{60})_mCu_n^-$ anions $(m \ge 2)$ is about a factor of 10^3 weaker than the yield of $(C_{60})_mCu_n^+$ cations. The difference in ion yield between cations and anions is even larger for $m = 0$ and 1; Cu_n^- and $C_{60}Cu_n^-$ are barely discernible in Figure 1b.

For a more quantitative comparison, we have determined the abundance of $(C_{60})_mCu_n^{\pm}$ ions from the mass spectra by a custom-designed software (briefly described in Section 2) that takes into account all possible isotopologues and contributions from impurities, background, and isotopologues of other ions.[32] Results are compiled in Figure 2 for cations and anions (left and right panels, respectively). Data for $(C_{60})_mCu_n^{\pm}$ for $0 \le m \le 3$ are displayed separately in the upper panels. Error bars indicate the 95% confidence interval; for most ions, they are smaller than the symbol size. The bottom panels display several representative stacked distributions for larger values of m. Distributions of cations that are not shown in panel 2e (i.e. for $m = 5, 7, 9, 10$) closely resemble distributions of similarly sized species that are shown. Distributions of anions with $7 \le m \le 10$ (not shown) are flat and featureless.

Abundance distributions of cations and anions extracted from mass spectra of HNDs doped with C_{60} and Au are displayed in Figure 3; they are arranged similarly to those in Figure 2 for copper. The vapor pressure of gold in the measurement of anions was significantly lower than in the measurement of cations, explaining the rapid decline in abundance with increasing n.

Close inspection of the mass spectrum of negatively charged C_{60}–copper complexes reveals the appearance of another series of mass peaks that are positioned exactly midway between peaks due to $(C_{60})_mCu_n^-$. Figure 4 shows sections of a mass spectrum starting with the bare fullerene monomer, dimer, and trimer (panels a, b, and c, respectively). Mass peaks due to $(C_{60})_mCu_n^-$ ($m = 1$, 2, and 3 in panels a, b, and c, respectively) are marked by full asterisks; open asterisks in panel c indicate peaks due to $(C_{60})_2Cu_n^-$.

DOI: 10.1021/acs.jpca.9b02768
J. Phys. Chem. A 2019, 123, 4599−4608

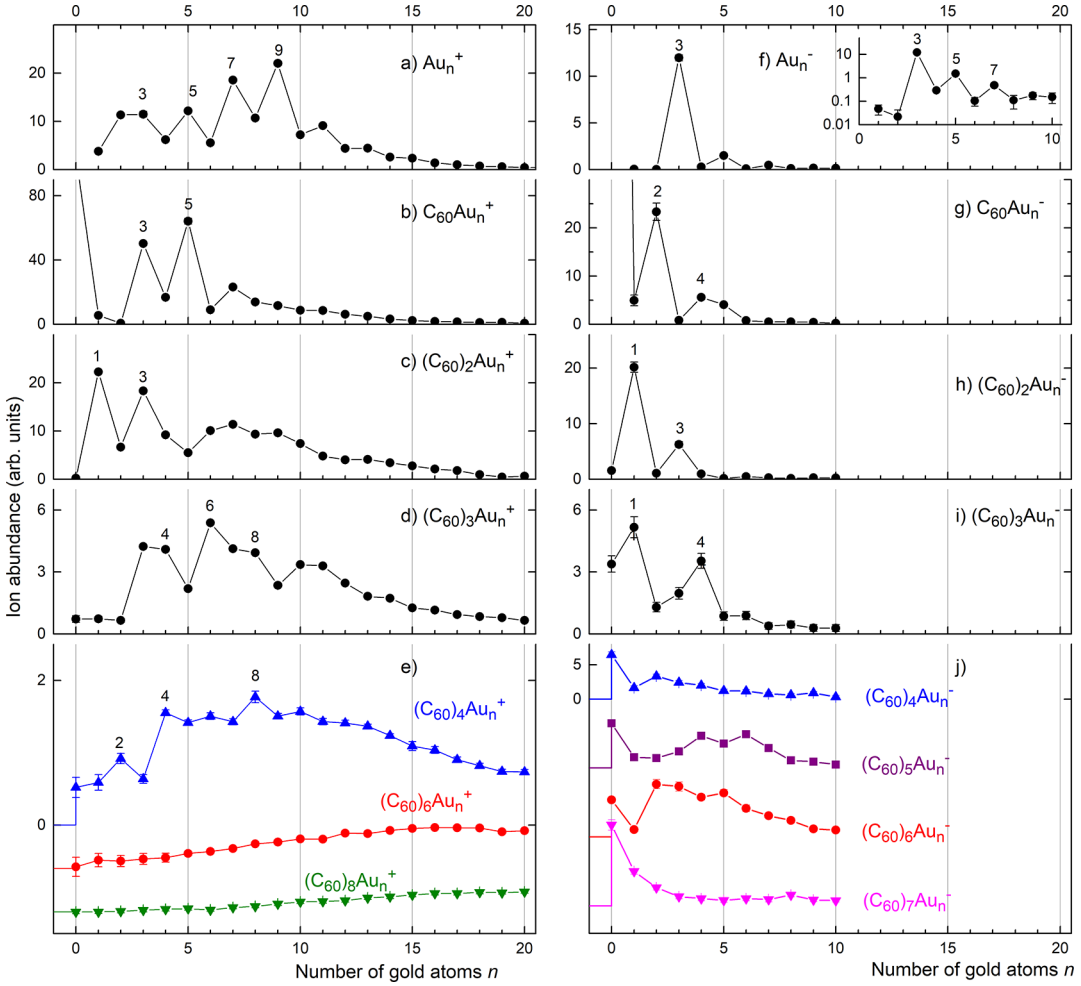

Figure 3. Abundance distributions of $(C_{60})_mAu_n^{\pm}$ $(0 \leq m \leq 3)$ cations and anions (left and right panels, respectively). Representative distributions for larger values of m in the bottom panels e and j are stacked; base lines are indicated by horizontal lines below $n = 0$.

The only other intense mass peaks in Figure 4 are the aforementioned peaks located midway between $(C_{60})_mCu_n^-$. Those positions are marked by vertical lines; corresponding mass peaks are most prominent near the center of panel b and toward the end of panel c. What is the nature of those mass peaks? A mass spectrometer measures the mass-to-charge- ratio of ions, hence mass peaks that are midway between $(C_{60})_mCu_n^-$ ions might be due to $(C_{60})_2Cu_n^{2-}$ dianions (n odd) in panel a, $(C_{60})_4Cu_n^{2-}$ in panel b, and $(C_{60})_6Cu_n^{2-}$ in panel c. The yield of these ions is statistically significant for $5 \leq n \leq 15$ (odd n) in panel a, $7 \leq n \leq 21$ in panel b, and $17 \leq n \leq 21$ in panel c.

A word of caution is in order, though. A definite proof of our assignment would require a comparison of the shape of each group of mass peaks with the characteristic pattern of $(C_{60})_mCu_n^{2-}$ isotopologues. Even more telling would be the identification of mass peaks at nominally half-integer mass because of dianions whose nominal mass number is odd. The statistical quality of the (strongly smoothed) mass spectrum shown in Figure 4 is insufficient for this task; acquisition of spectra with the required statistical quality is currently not feasible.

4. DISCUSSION

The abundance distributions in Figures 2 and 3 reveal several local anomalies (i.e., deviations from the envelope) that suggest anomalies in the stability of specific ions. We begin our discussion with pure copper or gold clusters. The evaporative model originally proposed by Klots provides a link between cluster abundance and cluster stability or, more specifically, their dissociation energy D_n (also referred to as evaporation or separation energy, i.e., the activation energy for loss of one monomer).[34] The model assumes that, on the time scale of mass spectrometric detection, the excess energy is randomized and that all cluster ions being observed have undergone at least one evaporation. The model was initially proposed for and tested with van der Waals or hydrogen-bound clusters for which ionization is followed by intramolecular reactions that release a large amount of energy, more than enough to rapidly shed several monomers.

This scenario is less obvious in the present case: the cohesive energies of bulk copper and gold are 3.49 and 3.81 eV,[35] respectively; it is possible to "softly" ionize bare coinage metal clusters without causing fragmentation.[36] However, electron ionization of a doped helium droplet releases a large amount of excess energy. For cations, the process starts with the formation of a He^+ ion in the droplet.[37,38] The positive charge may jump by resonant charge exchange to an adjacent helium atom. This hopping process is terminated either by the formation of He_2^+ or by charge transfer to the dopant. In the latter case, about 15−20 eV (the difference between the ionization energies of helium, 24.59 eV, and the dopant) will

DOI: 10.1021/acs.jpca.9b02768
J. Phys. Chem. A 2019, 123, 4599−4608

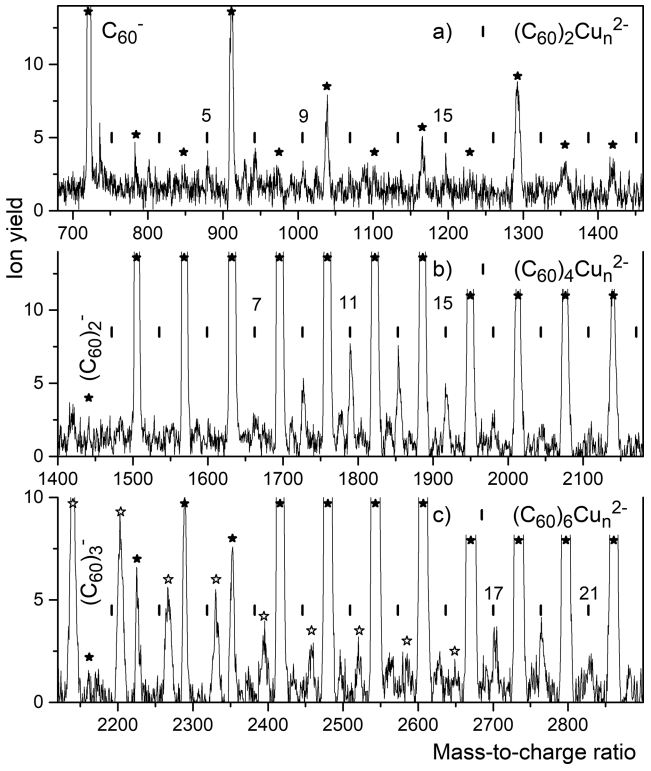

Figure 4. Three regions of a negative ion mass spectrum of HNDs doped with C_{60} and copper. Mass peaks due to singly charged $(C_{60})_mCu_n^-$ ions (m = 1, 2, and 3 in panels a, b, and c, respectively) are tracked by asterisks; open asterisks in panel c track peaks due to $(C_{60})_2Cu_n^-$. Vertical lines mark the expected positions of $(C_{60})_mCu_n^{2-}$ dianions with m = 2, 4, and 6, respectively, and odd values of n.

be released.[38,39] For anions, the dominant process starts with the inelastic scattering of an incident electron off a helium atom (producing electronically excited He*) and subsequent trapping of the thermalized electron in a bubble.[38,40] The threshold energy for this channel equals the sum of the threshold energies to form He* (19.8 eV) and the energy needed for the incident electron to penetrate the surface of the droplet (1.2 eV).[41] The slow electron can then attach to He* to form long-lived He^{*-} which may migrate to the dopant. Electron transfer to the dopant will release the energy stored in He^{*-} plus the electron affinity of the dopant. He^{*-} may also transfer two electrons to the dopant, thus forming dianions.[39]

Even if the basic assumption of the evaporative model is fulfilled, the link between cluster abundance and dissociation energy is intricate.[42,43] Deriving (relative) dissociation energies from measured abundance distributions involves several assumptions; see, for example, the analysis of water cluster cations and anions by Hansen et al.[44] Qualitatively, however, it is clear that an abrupt decrease of the dissociation energy (i.e. $D_{n+1} \ll D_n$) will cause an enrichment of cluster A_n at the expense of A_{n+1}. There are several different scenarios, such as a single cluster size that is particularly stable (a "magic" cluster) or particularly unstable with respect to its neighbors, or closure of a solvation shell, where D_n drops in a stepwise fashion. Their signatures in mass spectra will be different, but all of them are accompanied by abrupt changes in the abundance relative to the envelope of the abundance distribution. For simplicity, we will refer to cluster ions whose abundance is anomalously large relative to the next cluster size as "magic" or "particularly stable."

The abundances of pure, positively charged copper and gold clusters are presented in Figures 2a and 3a, respectively. According to the spherical jellium model, applicable to free-electron-like metals, the first two electronic shells (the 1s and 1p shell) are filled when the number of delocalized valence electrons in the (neutral or charged) cluster equals 2 and 8, respectively.[36,45] Electronic shell closure is accompanied by an abrupt drop of D_n. The abrupt drops in the measured abundance at n = 3 and 9 (already observed in previous work using different methods of cluster formation and ionization[46−49]) are consistent with this model. The observed odd−even alternation in the abundance, hence the stability of Cu_n^+ and Au_n^+ is another feature commonly observed for monovalent metal clusters, but its origin is not as obvious.[45,50]

The spherical jellium model is, of course, a gross simplification. Ion mobility measurements and density functional calculations reveal that Au_n^+ cluster ions are planar for $n \leq 7$.[51] Furthermore, the energetically preferred dissociation channel involves loss of Au atoms for even-numbered clusters but loss of Au_2 dimers from odd-numbered clusters (with the exception of Au_3^+). Even so, the size dependence of the computed adiabatic dissociation energies of the favored reaction channels display the abovementioned strong (factor two) odd−even effect, with particularly large values for Au_3^+ and Au_9^+.[51] Schweikhard, Hansen, and co-workers have measured dissociation energies of Au_n^+ by photofragmentation in the gas phase for $n \geq 7$; their values show similar trends.[52]

For negatively charged Cu and Au clusters, the number of atoms needed to fill the 1s and 1p shells (in the spherical jellium model) would be 1 and 7, respectively. The very low abundance of Cu_n^- anions (Figure 2f) precludes a critical analysis, but features consistent with the jellium model were observed in previous mass spectra of Cu_n^- anions formed by sputtering.[53,54] Note, however, that the odd-even effect in the data was stronger than the enhancement because of electronic shell closure.

The abundance distribution of Au_n^- anions (Figure 3f) features a striking maximum at n = 3; this ion is 2 orders of magnitude more abundant than the dimer and tetramer anion. The inset in Figure 3f displays the abundance of Au_n^- on a logarithmic scale; it reveals an odd−even oscillation with a hint of enhancement for Au_7^-. Previously reported abundance distributions of Au_n^- vary widely, from an envelope that decreases rapidly with increasing n to one described by a log-normal distribution peaking at roughly n = 10.[49,53] A common feature though is a strong odd−even oscillation, with odd-numbered sizes being more abundant. The enhancement of clusters that are predicted to be magic within the spherical jellium model (Au^- and Au_7^-) is weak at best, nor does Au_3^- appear to be magic in those earlier reports.

The special nature of Au_3^- is more obvious in mass spectra obtained by photoionization of gold clusters formed in a dc discharge at a gold cathode in a helium/argon flow.[55] Furthermore, the UPS spectrum of Au_3^- is quite unique and different from that of Cu_3^- and Ag_3^-.[55] Au_3^- has a particularly high (≈3.7 eV) vertical electron detachment energy, higher than any other ion below n = 9.[55−57] Ion mobility measurements and density functional calculations show that its lowest-energy structure is linear[58] (while clusters with $4 \leq n \leq 12$ are two-dimensional[57,59,60]). For energetically excited anions, there is always a competition between dissociation and electron detachment. When energetically allowed, photo-detachment is usually the dominant process and photo-

DOI: 10.1021/acs.jpca.9b02768
J. Phys. Chem. A 2019, 123, 4599−4608

fragmentation is a minor process.[55] Furthermore, the stability against evaporation of atoms from anions strongly correlates with the electron affinity of the neutral species.[54] Consequently, cluster anions with high detachment energies such as Au_3^- are likely to form magic numbers in mass spectra.

We now turn to a discussion of mixed clusters. We start with $(C_{60})_mAu_n^{\pm}$ because we have recently calculated dissociation channels for n, $m \leq 2$ and for $C_{60}Au_3^{\pm}$.[25] In fact, within this parameter space, all the maxima in computed energies for the most favorable reaction channels coincide with maxima in the corresponding ion abundance: for $C_{60}Au_n^+$, the dissociation energy is highest for $n = 3$, for $(C_{60})_2Au_n^+$, it is highest for $n = 1$, for $C_{60}Au_n^-$, it is highest for $n = 2$, for $(C_{60})_2Au_n^-$, it is highest for $n = 1$.

Given the excellent agreement between measured abundances and computed dissociation energies and our data in Figure 3, we conjecture that $C_{60}Au_5^+$, $C_{60}Au_4^-$, $(C_{60})_2Au_3^{\pm}$, $(C_{60})_3Au_4^{\pm}$, and $(C_{60})_3Au_8^+$ are particularly stable as well. These conjectures need to be confirmed by calculations which are beyond the scope of the current work.

The discussion so far misses important features in Figure 3, namely the nearly total absence of $(C_{60})_2^+$, $(C_{60})_2^-$, and $(C_{60})_3Au_n^+$ with $n = 0$, 1, and 2. Naively, bare $(C_{60})_m^{\pm}$ might be expected to form with high abundance as end products of long decay chains involving evaporation of Au atoms. (In experiments with very light metal doping, neutral pure $(C_{60})_x$ precursors would also populate the $(C_{60})_m^{\pm}$ ion series.) Mass spectra of fullerene clusters coated with He, H_2, O_2, N_2, H_2O, NH_3, CH_4, or C_2H_4 show this type of behavior.[61,62] However, $(C_{60})_mAu_n^{\pm}$ ions feature a competing dissociation channel, namely loss of a neutral or charged C_{60}. Our recent DFT study shows that this channel is energetically favored over emission of Au. In most cases, a charged C_{60} is lost, only $C_{60}Au_3^{\pm}$ emits a neutral C_{60} because of the high stability of $Au_3^{\pm}$.[25] The preference of $(C_{60})_2Au^+$ to emit C_{60}^+ combined with the absence of $(C_{60})_3^+$ (see Figure 2d) explains the absence of $(C_{60})_2^+$; there is no dissociation channel that feeds $(C_{60})_2^+$.

Another interesting example is $(C_{60})_3Au_2^+$, which is barely discernible although its two potential precursors, $(C_{60})_3Au_3^+$ and $(C_{60})_4Au_2^+$, are abundant (Figure 3d). In the absence of any theoretical work, what can we conclude? Presumably, $(C_{60})_3Au_3^+$ does not evaporate Au, instead it may dissociate into either $(C_{60})_2Au_3 + C_{60}^+$ or $(C_{60})_2Au_3^+ + C_{60}$. $(C_{60})_4Au_2^+$, on the other hand, probably does not emit C_{60}; it probably emits C_{60}^+ instead.

Of course, reality may be more complicated. Rapid sequential emission of two monomers from the above-mentioned precursor ions might render an intermediate $(C_{60})_3Au_2^+$ ion undetectable (if, e.g., emission of Au from $(C_{60})_3Au_3^+$ was to be followed by a rapid emission of C_{60} or C_{60}^+). One may also have to consider dissociation into two clusters rather than sequential emission of two monomers. These channels are less common, but they do occur. For example, metastable C_{60}^+ undergoes unimolecular dissociation by sequential emission of two C_2 units on a time scale of 10 μs,[63] and monovalent metal cluster ions such as Na_n^+ or Au_n^+ feature competition between monomer and dimer loss for certain values of n.[51,52,64]

For anions, one should also consider the possibility of electron detachment. The channel is not likely to become competitive for pure, large Au_n^- because the detachment energy converges to the work function (4.82 eV),[35] whereas the dissociation energy converges to the lower (3.81 eV)[35] cohesive energy.

Above we mentioned that the energetically most facile dissociation channel of small $(C_{60})_mAu_n^+$ (m, $n \leq 2$) is the emission of a charged C_{60}^+.[25] Evaporation of charged monomers is highly unusual. For homogeneous cluster ions, this channel is closed because the ionization energy tends to decrease with increasing size; energetics thus favor emission of a neutral monomer. A preference for emission of C_{60}^+ over C_{60} implies that for m, $n \leq 2$, the ionization energy of the neutral fragment exceeds 7.58 eV, the ionization energy of C_{60}.[65] In our previous work,[25] we have reported the dissociation energies for both channels, hence the ionization energies of the neutral fragments can be derived.[66] It is smallest for $(C_{60})_2Au$, with a value of 7.73 eV. There is no obvious way to estimate how the ionization energy of $(C_{60})_mAu_n$ will change with increasing size m, n. Eventually though, we expect that evaporation of C_{60} will be favored over evaporation of C_{60}^+.

However, how about emission of (neutral or charged) Au as opposed to C_{60}? Will Au loss become competitive for larger complexes? Definitely yes if gold coats C_{60} as predicted in the first-principles study by Batista et al.[24] The calculated binding energy of C_{60} to a complete gold shell containing 92 atoms is 4.46 eV, larger than the cohesive energy of gold (3.81 eV). Even partial wetting may tip the balance in favor of Au loss; the layer may also cage the fullerene.

However, the results of Batista's study are conflicting with other work. True, some metals (including the alkaline earth metals) do wet C_{60};[28,68] thulium and holmium even seem to coat individual C_{60} within a (positively charged) fullerene aggregate.[69] The experimental evidence pertaining to gold is scarce and rather indirect. Palpant et al. have recorded UPS data of $C_{60}Au_n^-$ ($n \leq 6$) in the gas phase.[17] The detachment energies exhibited the same odd−even oscillation as for pure Au_n^-, which in turn conforms to the electronic shell model.[56] Palpant et al. concluded that Au atoms preferably form a Au_n cluster on the fullerene cage rather than a layered structure spread over the cage. Kröger et al. have deposited Au on films of C_{60} and recorded UPS and XPS data.[9] They concluded that gold clusters do not nucleate at specific nucleation sites such as dimples, which would be the preferred sites for physisorbed species.[70] The smallest gold clusters created in the experiment, even at lowest coverage, consisted of approximately 50 Au atoms.[9]

The experimental evidence summarized in the previous paragraph may be insufficient to rule out that gold wets C_{60}, but our recent theoretical work[25] clearly does. The ground-state structures computed for small $(C_{60})_mAu_n^{\pm}$ were approximately linear and independent of charge state for complexes with n, $m \leq 2$; their structures may be characterized as $C_{60}AuAu^{\pm}$, $C_{60}AuC_{60}^{\pm}$, and $C_{60}AuAuC_{60}^{\pm}$. The only exception was $C_{60}Au_3^{\pm}$, which has a triangular gold cluster with the C_{60} bound to one of its apex atoms.[25] Moreover, the interaction was covalent with dissociation energies for loss of neutral or charged C_{60} ranging from 0.5 eV to 1.7 eV, much larger than the value (≈0.05 eV per gold atom) computed by Batista et al.[24] Those authors also obtained large bond lengths (≈3.6 Å) for the gold atoms, which were found to be bound atop carbon atoms. We also found the atop site to be lowest in energy for $C_{60}Au^{\pm}$, but the bond length is only ≈2.2 Å.[25] A similar bond length was obtained in a DFT study of neutral $C_{60}Au$ and symmetry-constrained linear $AuAu-C_{60}-AuAu$.[20,23]

DOI: 10.1021/acs.jpca.9b02768
J. Phys. Chem. A 2019, 123, 4599−4608

Our discussion now turns to copper. The absence of $(C_{60})_2^{\pm}$ and $(C_{60})_3Cu_n^+$ (n = 0, 1, and 2) cations and the local maxima for $(C_{60})_2Cu^{\pm}$ mirror the results for C_{60}–gold complexes. On the other hand, the near-absence of $(C_{60})_3Cu_n^-$ anions (n = 0, 1, 2, and 3) contrasts with the high abundance of $(C_{60})_3Au^-$. In addition, the apparent preference for even-numbered $(C_{60})_2Cu_n^+$ (n = 4, 6, 8, 10) looks a lot like the preference for even-numbered $(C_{60})_3Au_n^+$ (n = 4, 6, 8).

Another interesting feature is the sudden change from a highly structured distribution for $(C_{60})_2Cu_n^+$ to a smooth one for $(C_{60})_3Cu_n^+$ (for C_{60}–gold complexes, a similar change occurs much later, from m = 4 to 5). What causes this sudden change, and the difference between copper and gold? For a possible clue, let us consider previous reports on the copper–C_{60} system. Electron spin resonance spectra of C_{60} films doped with copper indicate the formation of C_{60}^{z-} anions in high (z > 1) charge states that are stable at 500 °C.[71] Robledo et al. have explored $C_{60}Cu^+$ with DFT.[19] They find that the most favorable adsorption site of Cu is a bridge site between two hexagonal rings, with an adsorption energy of about 3.0 eV, twice the value computed by us for $C_{60}Au^+$, which prefers the atop site.[25] A natural population analysis shows that the net charge of $C_{60}Cu^+$ is mainly localized on the copper atom; charge analysis of the carbon atoms indicates a very localized interaction between Cu^+ and the two carbon atoms that define the bridge position.[19]

The strong $C_{60}Cu^+$ bond energy may favor evaporation of copper atoms (as opposed to C_{60}) if a distinct copper cluster forms at all. Furthermore, the cohesive energy of copper is 0.32 eV lower than that of gold, also favoring evaporation of metal atoms for copper as compared with gold. However, in that scenario, one would expect magic numbers that are reminiscent of those of bare copper clusters, the opposite of what we are observing. A smooth distribution may also be expected if the copper atoms are dispersed on a cluster of fullerenes, that is, if copper wets C_{60}. C_{60} wetted by other metals (alkalis, alkaline earths, thulium, and holmium) exhibits magic numbers as well but at sizes larger than those covered in the present work.[28,69]

Perhaps the only firm conclusion that we can draw at this point is that for both charge states and both metals, $(C_{60})_2Cu^{\pm}$ and $(C_{60})_2Au^{\pm}$ favor loss of a (neutral or charged) fullerene over loss of the metal atom (emission of a charged metal atom can be safely excluded on energetic grounds). For the C_{60} trimer, a similar trend exists, but there are also distinct differences between the charge states, and between copper and gold.

Finally, we briefly discuss the appearance of $(C_{60})_mCu_n^{2-}$ dianions with m = 2, 4, and 6 and n odd. The observation of C_{60}^{2-} dianions in the gas phase was first reported in 1991.[72,73] The calculated adiabatic electron affinity of C_{60}^- is slightly negative, that is, the dianion is metastable, consistent with its finite lifetime measured in a storage ring.[74,75] In contrast, clusters of C_{60} are expected to form stable dianions because the Coulomb repulsion between the excess electrons decreases while the polarizability of the system increases with cluster size.[76,77]

Thus, the present observation of $(C_{60})_mCu_n^{2-}$ dianions with $m \geq 2$ is not surprising, but the formation mechanism deserves a discussion. In the gas phase, sequential attachment of one or more electrons to an anion is impeded by the repulsive Coulomb barrier for the incoming electron(s). Schweikhard and co-workers have managed to sequentially add up to five electrons to aluminum clusters (containing about 450 atoms) by judiciously adjusting the electric potential of their ion trap.[78] As discussed above, dianions can be formed in helium droplets by a single incident electron via formation of an intermediate He^{*-}, which subsequently transfers two electrons to the dopant.[39] In our previous work,[39] C_{60} pentamers were the smallest observed dianions while in the current work, we observe $(C_{60})_mCu_n^{2-}$ dianions with $m \geq 2$. The difference is possibly due to different dopant levels of the HNDs, but the presence of metal atoms and the concomitant increase in the stability of dianions may also play a role.

Surprisingly, we do not observe $(C_{60})_mCu_n^{2-}$ dianions with odd values of m. Their mass peaks would be positioned close to singly charged $(C_{60})_pCu_q^-$ ions (p, q = integer) but still visible if they were as abundant as doubly charged ions with m = 4 and 6 in panels b and c, respectively. We cannot offer a compelling explanation for this odd–even effect. In our previous work, we identified only odd-numbered $(C_{60})_m^{2-}$ dianions because even-numbered $(C_{60})_m^{2-}$ are hidden under the mass peaks of singly charged $(C_{60})_{m/2}^-$ anions.[39] We note that Zettergren et al. observed an odd–even effect in the ionization cross sections of C_{60} dimers $(C_{60})_2^{z+}$, which was tentatively explained with a geometrical argument, but the oscillation versus charge state z in that work bears no obvious relation to the apparent oscillation in the abundance of $(C_{60})_mCu_n^{2-}$ versus size m. More work is needed to identify the nature of the perceived odd–even effect in our present data.

5. CONCLUSIONS

We have synthesized clusters of C_{60} and gold or copper in HNDs and recorded mass spectra of positive and negative ions formed by electron ionization. $(C_{60})_mM_n^{\pm}$ ions containing several fullerenes and metal atoms (M = Cu or Au) were observed. Their abundance distributions, presented here versus n for fixed values of m, feature several local anomalies. For small $(C_{60})_mAu_n^{\pm}$, the observed abundance anomalies agree with sizes previously calculated to be particularly stable,[25] confirming the direct if qualitative correlation between abundance distributions and stability. Another feature, the absence of bare C_{60} dimers of either charge state, is also consistent with the previous theoretical study because it implies that $(C_{60})_2M^{\pm}$ does not dissociate by loss of a neutral metal atom.

$(C_{60})_3M_n^+$ ions are absent for n = 0, 1, and 2 but present for n = 3. We conclude that $(C_{60})_3M_3^+$ does not dissociate by neutral atom loss. Ejection of the stable M_3^+ is a likely channel as previously computed for $C_{60}Au_3^+$. On the other hand, the abundance distributions of $(C_{60})_3Cu_n^-$ and $(C_{60})_3Au_n^-$ anions are dissimilar, possibly because of differences in the fragmentation channels that lead to these ions. Theoretical work is needed to better understand the origin of similarities and differences between cations and anions, and between copper and gold.

It would be highly desirable to directly identify the ions produced by unimolecular dissociation. Time-of-flight mass spectrometers equipped with a reflectron are, in general, well suited for that task.[79] Unfortunately, the commercial high-resolution instrument used in the present work does not offer the flexibility for that type of analysis.

Also needed are theoretical studies of complexes larger than $(C_{60})_2M_2^{\pm}$. The predicted[25] structure of $(C_{60})_2Au_2^{\pm}$, with Au_2 sandwiched between two C_{60} in a linear arrangement, cannot

DOI: 10.1021/acs.jpca.9b02768
J. Phys. Chem. A 2019, 123, 4599–4608

be categorized as a *wet* or *dry* structure. How would another C_{60} bind to that complex? Another gold atom? Does copper form similar structures? Hopefully, the experimental data presented here will stimulate work that addresses these questions.

AUTHOR INFORMATION

Corresponding Authors

*E-mail: paul.scheier@uibk.ac.at (P.S.).
*E-mail: olof.echt@unh.edu (O.E.).

ORCID

Paul Scheier: 0000-0002-7480-6205
Olof Echt: 0000-0002-0970-1191

Notes

The authors declare no competing financial interest.

ACKNOWLEDGMENTS

This work was supported by the Austrian Science Fund (FWF) Wien (project numbers P26635, P31149, and W1259) and the European Commission (ELEvaTE H2020 Twinning Project, project number 692335).

REFERENCES

(1) Kroto, H. W.; Heath, J. R.; O'Brien, S. C.; Curl, R. F.; Smalley, R. E. C_{60}: Buckminsterfullerene. *Nature* **1985**, *318*, 162−163.
(2) Rosseinsky, M. J. Recent Developments in the Chemistry and Physics of Metal Fullerides. *Chem. Mater.* **1998**, *10*, 2665−2685.
(3) Yoon, M.; Yang, S. Y.; Hicke, C.; Wang, E.; Geohegan, D.; Zhang, Z. Y. Calcium as the Superior Coating Metal in Functionalization of Carbon Fullerenes for High-Capacity Hydrogen Storage. *Phys. Rev. Lett.* **2008**, *100*, 206806.
(4) Wang, Q.; Jena, P. Density Functional Theory Study of the Interaction of Hydrogen with Li_6C_{60}. *J. Phys. Chem. Lett.* **2012**, *3*, 1084−1088.
(5) Robledo, M.; Díaz-Tendero, S.; Martín, F.; Alcamí, M. Theoretical Study of the Interaction between Molecular Hydrogen and MC_{60}^+ Complexes. *RSC Adv.* **2016**, *6*, 27447−27451.
(6) Kaiser, A.; Renzler, M.; Kranabetter, L.; Schwärzler, M.; Parajuli, R.; Echt, O.; Scheier, P. On Enhanced Hydrogen Adsorption on Alkali (Cesium) Doped C_{60} and Effects of the Quantum Nature of the H_2 Molecule on Physisorption Energies. *Int. J. Hydrogen Energy* **2017**, *42*, 3078−3086.
(7) Lebedeva, M. A.; Chamberlain, T. W.; Khlobystov, A. N. Harnessing the Synergistic and Complementary Properties of Fullerene and Transition-Metal Compounds for Nanomaterial Applications. *Chem. Rev.* **2015**, *115*, 11301−11351.
(8) Chen, Y.-C.; Hsu, C.-Y.; Lin, R. Y.-Y.; Ho, K.-C.; Lin, J. T. Materials for the Active Layer of Organic Photovoltaics: Ternary Solar Cell Approach. *ChemSusChem* **2013**, *6*, 20−35.
(9) Kröger, H.; Reinke, P.; Büttner, M.; Oelhafen, P. Gold Cluster Formation on a Fullerene Surface. *J. Chem. Phys.* **2005**, *123*, 114706.
(10) Liu, W.; Gao, X. Reducing $HAuCl_4$ by the C_{60} Dianion: C_{60}-Directed Self-Assembly of Gold Nanoparticles into Novel Fullerene Bound Gold Nanoassemblies. *Nanotechnology* **2008**, *19*, 405609.
(11) Ren, Y.; Paira, P.; Nayak, T. R.; Ang, W. H.; Pastorin, G. Synthesis of Fullerene@Gold Core-Shell Nanostructures. *Chem. Commun.* **2011**, *47*, 7710−7712.
(12) Xie, Y.-c.; Fard, M. R.; Kaya, D.; Bao, D.; Palmer, R. E.; Du, S.; Guo, Q. Site-Specific Assembly of Fullerene Nanorings Guided by Two-Dimensional Gold Clusters. *J. Phys. Chem. C* **2016**, *120*, 10975−10981.
(13) Kaya, D.; Gao, J.; Fard, M. R.; Palmer, R. E.; Guo, Q. Controlled Manipulation of Magic Number Gold-Fullerene Clusters Using Scanning Tunneling Microscopy. *Langmuir* **2018**, *34*, 8388−8392.
(14) Xiao, W.; Zhang, W. Synthesis and characterization of hybrid materials formed by C_{60} in situ decorating copper clusters. *Mater. Lett.* **2007**, *61*, 1064−1067.
(15) Singhal, R.; Gupta, S.; Vishnoi, R.; Singh, D.; Sharma, G. D. Study on Copper-Fullerene Nanocomposite Irradiated by 120 MeV Au Ions. *Radiat. Phys. Chem.* **2018**, *151*, 276−282.
(16) Yoshikawa, G.; Tsuruma, Y.; Ikeda, S.; Saiki, K. Noble Metal Intercalated Fullerene Fabricated by Low-Temperature Co-Deposition. *Adv. Mater.* **2010**, *22*, 43−46.
(17) Palpant, B.; Negishi, Y.; Sanekata, M.; Miyajima, K.; Nagao, S.; Judai, K.; Rayner, D. M.; Simard, B.; Hackett, P. A.; Nakajima, A.; et al. Electronic and Geometric Properties of Exohedral Sodium- and Gold-Fullerenes. *J. Chem. Phys.* **2001**, *114*, 8459−8466.
(18) Lyon, J. T.; Andrews, L. Infrared Spectrum of the Au-C_{60} Complex. *ChemPhysChem* **2005**, *6*, 229−232.
(19) Robledo, M.; Aguirre, N. F.; Díaz-Tendero, S.; Martín, F.; Alcamí, M. Bonding in Exohedral Metal-Fullerene Cationic Complexes. *RSC Adv.* **2014**, *4*, 53010−53020.
(20) Zeng, Q.; Chu, X.; Yang, M.; Wu, D.-Y. Spin-Orbit Coupling Effect on Au-C_{60} Interaction: A Density Functional Theory Study. *Chem. Phys.* **2012**, *395*, 82−86.
(21) Shukla, M. K.; Dubey, M.; Leszczynski, J. Theoretical Investigation of Electronic Structures and Properties of C_{60}−Gold Nanocontacts. *ACS Nano* **2008**, *2*, 227−234.
(22) Shukla, M. K.; Dubey, M.; Zakar, E.; Leszczynski, J. Density Functional Theory Investigation of Electronic Structures and Properties of Ag_n-C_{60}-Ag_n Nanocontacts. *J. Phys. Chem. C* **2012**, *116*, 1966−1972.
(23) Zeng, Q.; Chu, X.; Wang, X.; Yang, M. First-Principles Study of AuC_{60} Clusters. *J. Nanosci. Nanotechnol.* **2012**, *12*, 6571−6575.
(24) Batista, R. J. C.; Mazzoni, M. S. C.; Ladeira, L. O.; Chacham, H. First-Principles Investigation of Au-Covered Carbon Fullerenes. *Phys. Rev. B: Condens. Matter Mater. Phys.* **2005**, *72*, 085447.
(25) Goulart, M.; Kuhn, M.; Martini, P.; Chen, L.; Hagelberg, F.; Kaiser, A.; Scheier, P.; Ellis, A. M. Highly Stable $[C_{60}AuC_{60}]^{+/-}$ Dumbbells. *J. Phys. Chem. Lett.* **2018**, *9*, 2703−2706.
(26) Pyykkö, P. Predicted Chemical Bonds between Rare Gases and Au^+. *J. Am. Chem. Soc.* **1995**, *117*, 2067−2070.
(27) Wang, L.-S. Covalent Gold. *Phys. Chem. Chem. Phys.* **2010**, *12*, 8694−8705.
(28) Zimmermann, U.; Malinowski, N.; Burkhardt, A.; Martin, T. P. Metal-Coated Fullerenes. *Carbon* **1995**, *33*, 995−1006.
(29) Renzler, M.; Kranabetter, L.; Goulart, M.; Scheier, P.; Echt, O. Positively and Negatively Charged Cesium and $(C_{60})_mCs_n$ Cluster Ions. *J. Phys. Chem. C* **2017**, *121*, 10817−10823.
(30) Gomez, L. F.; Loginov, E.; Sliter, R.; Vilesov, A. F. Sizes of Large He Droplets. *J. Chem. Phys.* **2011**, *135*, 154201.
(31) An der Lan, L.; Bartl, P.; Leidlmair, C.; Schöbel, H.; Jochum, R.; Denifl, S.; Märk, T. D.; Ellis, A. M.; Scheier, P. The Submersion of Sodium Clusters in Helium Nanodroplets: Identification of the Surface → Interior Transition. *J. Chem. Phys.* **2011**, *135*, 044309.
(32) Ralser, S.; Postler, J.; Harnisch, M.; Ellis, A. M.; Scheier, P. Extracting Cluster Distributions from Mass Spectra: Isotopefit. *Int. J. Mass Spectrom.* **2015**, *379*, 194−199.
(33) Kaiser, A.; Leidlmair, C.; Bartl, P.; Zöttl, S.; Denifl, S.; Mauracher, A.; Probst, M.; Scheier, P.; Echt, O. Adsorption of Hydrogen on Neutral and Charged Fullerene: Experiment and Theory. *J. Chem. Phys.* **2013**, *138*, 074311.
(34) Klots, C. E. The Evaporative Ensemble. *Z. Phys. D: At., Mol. Clusters* **1987**, *5*, 83−89.
(35) http://www.knowledgedoor.com/ (accessed Nov 5, 2018).
(36) De Heer, W. A. The Physics of Simple Metal Clusters: Experimental Aspects and Simple Models. *Rev. Mod. Phys.* **1993**, *65*, 611−676.
(37) Ellis, A. M.; Yang, S. F. Model for the Charge-Transfer Probability in Helium Nanodroplets Following Electron-Impact Ionization. *Phys. Rev. A: At., Mol., Opt. Phys.* **2007**, *76*, 032714.
(38) Mauracher, A.; Echt, O.; Ellis, A. M.; Yang, S.; Bohme, D. K.; Postler, J.; Kaiser, A.; Denifl, S.; Scheier, P. Cold Physics and

DOI: 10.1021/acs.jpca.9b02768
J. Phys. Chem. A 2019, 123, 4599−4608

Chemistry: Collisions, Ionization and Reactions inside Helium Nanodroplets Close to Zero K. *Phys. Rep.* **2018**, *751*, 1−90.
(39) Mauracher, A.; Daxner, M.; Huber, S. E.; Postler, J.; Renzler, M.; Denifl, S.; Scheier, P.; Ellis, A. M. The interaction of He^- with fullerenes. *J. Chem. Phys.* **2015**, *142*, 104306.
(40) Mauracher, A.; Daxner, M.; Postler, J.; Huber, S. E.; Denifl, S.; Scheier, P.; Toennies, J. P. Detection of Negative Charge Carriers in Superfluid Helium Droplets: The Metastable Anions He^{*-} and He_2^{*-}. *J. Phys. Chem. Lett.* **2014**, *5*, 2444−2449.
(41) Direct attachment of the incident electron to the dopant is another process, and the only viable process for electron energies below 21 eV. However, this process is statistically unlikely in large droplets.
(42) Casero, R.; Soler, J. M. Onset and evolution of "magic numbers" in mass spectra of molecular clusters. *J. Chem. Phys.* **1991**, *95*, 2927−2935.
(43) Hansen, K. *Statistical Physics of Nanoparticles in the Gas Phase*. Springer, 2012; Vol. 73.
(44) Hansen, K.; Andersson, P. U.; Uggerud, E. Activation Energies for Evaporation from Protonated and Deprotonated Water Clusters from Mass Spectra. *J. Chem. Phys.* **2009**, *131*, 124303.
(45) Brack, M. The physics of simple metal clusters: self-consistent jellium model and semiclassical approaches. *Rev. Mod. Phys.* **1993**, *65*, 677−732.
(46) Katakuse, I.; Ichihara, T.; Fujita, Y.; Matsuo, T.; Sakurai, T.; Matsuda, H. Mass Distributions of Copper, Silver and Gold Clusters and Electronic Shell Structure. *Int. J. Mass Spectrom. Ion Processes* **1985**, *67*, 229−236.
(47) Rabin, I.; Jackschath, C.; Schulze, W. Shell Effects in Singly and Multiply Charged Silver and Gold Clusters. *Z. Phys. D: At., Mol. Clusters* **1991**, *19*, 153−155.
(48) Becker, S.; Dietrich, G.; Hasse, H.-U.; Klisch, N.; Kluge, H.-J.; Kreisle, D.; Krückeberg, S.; Lindinger, M.; Lützenkirchen, K.; Schweikhard, L.; et al. Collision induced dissociation of stored gold cluster ions. *Z. Phys. D: At., Mol. Clusters* **1994**, *30*, 341−348.
(49) Martini, P.; Kranabetter, L.; Goulart, M.; Kuhn, M.; Gatchell, M.; Bohme, D. K.; Scheier, P. Formation of Positive and Negative Clusters of Gold Atoms inside Helium Nanodroplets Close to Zero K. *Int. J. Mass Spectrom.* **2018**, *434*, 136−141.
(50) Yannouleas, C.; Landman, U. Electronic shell effects in triaxially deformed metal clusters: A systematic interpretation of experimental observations. *Phys. Rev. B: Condens. Matter Mater. Phys.* **1995**, *51*, 1902−1917.
(51) Gilb, S.; Weis, P.; Furche, F.; Ahlrichs, R.; Kappes, M. M. Structures of Small Gold Cluster Cations (Au_n^+, $n < 14$): Ion Mobility Measurements Versus Density Functional Calculations. *J. Chem. Phys.* **2002**, *116*, 4094−4101.
(52) Hansen, K.; Herlert, A.; Schweikhard, L.; Vogel, M. Dissociation Energies of Gold Clusters Au_N^+, N=7-27. *Phys. Rev. A: At., Mol., Opt. Phys.* **2006**, *73*, 063202.
(53) Katakuse, I.; Ichihara, T.; Fujita, Y.; Matsuo, T.; Sakurai, T.; Matsuda, H. Mass Distributions of Negative Cluster Ions of Copper, Silver and Gold. *Int. J. Mass Spectrom. Ion Processes* **1986**, *74*, 33−41.
(54) Hansen, K.; Andersen, J. U.; Forster, J. S.; Hvelplund, P. Formation and Fragmentation of Negative Metal Clusters. *Phys. Rev. A: At., Mol., Opt. Phys.* **2001**, *63*, 023201.
(55) Ho, J.; Ervin, K. M.; Lineberger, W. C. Photoelectron Spectroscopy of Metal Cluster Anions: Cu_n^-, Ag_n^-, and Au_n^-. *J. Chem. Phys.* **1990**, *93*, 6987−7002.
(56) Taylor, K. J.; Pettiette-Hall, C. L.; Cheshnovsky, O.; Smalley, R. E. Ultraviolet Photoelectron Spectra of Coinage Metal Clusters. *J. Chem. Phys.* **1992**, *96*, 3319−3329.
(57) Häkkinen, H.; Yoon, B.; Landman, U.; Li, X.; Zhai, H.-J.; Wang, L.-S. On the Electronic and Atomic Structures of Small Au_N^- (N = 4-14) Clusters: A Photoelectron Spectroscopy and Density-Functional Study. *J. Phys. Chem. A* **2003**, *107*, 6168−6175.
(58) Furche, F.; Ahlrichs, R.; Weis, P.; Jacob, C.; Gilb, S.; Bierweiler, T.; Kappes, M. M. The Structures of Small Gold Cluster Anions as Determined by a Combination of Ion Mobility Measurements and Density Functional Calculations. *J. Chem. Phys.* **2002**, *117*, 6982−6990.
(59) Johansson, M. P.; Lechtken, A.; Schooss, D.; Kappes, M. M.; Furche, F. 2d-3d Transition of Gold Cluster Anions Resolved. *Phys. Rev. A: At., Mol., Opt. Phys.* **2008**, *77*, 053202.
(60) Liao, M.-S.; Watts, J. D.; Huang, M.-J. Theoretical Comparative Study of Oxygen Adsorption on Neutral and Anionic Ag_n and Au_n Clusters (n = 2-25). *J. Phys. Chem. C* **2014**, *118*, 21911−21927.
(61) Zöttl, S.; Kaiser, A.; Daxner, M.; Goulart, M.; Mauracher, A.; Probst, M.; Hagelberg, F.; Denifl, S.; Scheier, P.; Echt, O. Ordered Phases of Ethylene Adsorbed on Charged Fullerenes and Their Aggregates. *Carbon* **2014**, *69*, 206−220.
(62) Echt, O.; Kaiser, A.; Zöttl, S.; Mauracher, A.; Denifl, S.; Scheier, P. Adsorption of Polar and Non-Polar Molecules on Isolated Cationic C_{60}, C_{70}, and Their Aggregates. *ChemPlusChem* **2013**, *78*, 910−920.
(63) Foltin, M.; Echt, O.; Scheier, P.; Dünser, B.; Wörgötter, R.; Muigg, D.; Matt, S.; Märk, T. D. Dissociation of Singly and Multiply Charged Fullerenes: Emission of C_4, or Sequential Emission of C_2? *J. Chem. Phys.* **1997**, *107*, 6246−6256.
(64) Bréchignac, C.; Cahuzac, P.; Leygnier, J.; Weiner, J. Dynamics of unimolecular dissociation of sodium cluster ions. *J. Chem. Phys.* **1989**, *90*, 1492−1498.
(65) de Vries, J.; Steger, H.; Kamke, B.; Menzel, C.; Weisser, B.; Kamke, W.; Hertel, I. V. Single-Photon Ionization of C_{60}- and C_{70}-Fullerene with Synchrotron Radiation: Determination of the Ionization Potential of C_{60}. *Chem. Phys. Lett.* **1992**, *188*, 159−162.
(66) Similarly, small $(C_{60})_mAu_n^-$ (m, $n \leq 2$) are predicted to emit C_{60}^-.[25] Hence the electron affinities of their neutral fragments must be below 2.6835, the electron affinity of C_{60}.[67] Values can be derived from dissociation energies of the anions computed for the competing channels.[25]
(67) Huang, D.-L.; Dau, P. D.; Liu, H.-T.; Wang, L.-S. High-Resolution Photoelectron Imaging of Cold C_{60}^- Anions and Accurate Determination of the Electron Affinity of C_{60}. *J. Chem. Phys.* **2014**, *140*, 224315.
(68) Zimmermann, U.; Malinowski, N.; Näher, U.; Frank, S.; Martin, T. P. Multilayer Metal Coverage of Fullerene Molecules. *Phys. Rev. Lett.* **1994**, *72*, 3542−3545.
(69) Malinowski, N.; Branz, W.; Billas, I. M. L.; Heinebrodt, M.; Tast, F.; Martin, T. P. Cluster Assemblies of Metal-Coated Fullerenes. *Eur. Phys. J. D* **1999**, *9*, 41−44.
(70) Kaiser, A.; Zöttl, S.; Bartl, P.; Leidlmair, C.; Mauracher, A.; Probst, M.; Denifl, S.; Echt, O.; Scheier, P. Methane Adsorption on Aggregates of Fullerenes: Site-Selective Storage Capacities and Adsorption Energies. *ChemSusChem* **2013**, *6*, 1235−1244.
(71) Solodovnikov, S. P. ESR Studies of Doping C_{60} Fullerene by Zinc, Cadmium, Copper, Gallium, and Indium Vapors. *Russ. Chem. Bull.* **1997**, *46*, 289−291.
(72) Hettich, R. L.; Compton, R. N.; Ritchie, R. H. Doubly Charged Negative Ions of Carbon-60. *Phys. Rev. Lett.* **1991**, *67*, 1242.
(73) Limbach, P. A.; Schweikhard, L.; Cowen, K. A.; McDermott, M. T.; Marshall, A. G.; Coe, J. V. Observation of the Doubly Charged, Gas-Phase Fullerene Anions C_{60}^{2-} and C_{70}^{2-}. *J. Am. Chem. Soc.* **1991**, *113*, 6795−6798.
(74) Zettergren, H.; Alcami, M.; Martin, F. First- and Second-Electron Affinities of C_{60} and C_{70} Isomers. *Phys. Rev. A: At., Mol., Opt. Phys.* **2007**, *76*, 043205.
(75) Tomita, S.; Andersen, J. U.; Cederquist, H.; Concina, B.; Echt, O.; Forster, J. S.; Hansen, K.; Huber, B. A.; Hvelplund, P.; Jensen, J.; et al. Lifetimes of C_{60}^{2-} and C_{70}^{2-} Dianions in a Storage Ringe. *J. Chem. Phys.* **2006**, *124*, 024310.
(76) Shubina, T. E.; Sharapa, D. I.; Schubert, C.; Zahn, D.; Halik, M.; Keller, P. A.; Pyne, S. G.; Jennepalli, S.; Guldi, D. M.; Clark, T. Fullerene Van Der Waals Oligomers as Electron Traps. *J. Am. Chem. Soc.* **2014**, *136*, 10890−10893.
(77) Voora, V. K.; Jordan, K. D. Nonvalence Correlation-Bound Anion States of Spherical Fullerenes. *Nano Lett.* **2014**, *14*, 4602−4606.

DOI: 10.1021/acs.jpca.9b02768
J. Phys. Chem. A 2019, 123, 4599−4608

(78) Martinez, F.; Bandelow, S.; Breitenfeldt, C.; Marx, G.; Schweikhard, L.; Wienholtz, F.; Ziegler, F. Lifting of the Trapping Potential During Ion Storage for Multi-Anion Production in a Penning Trap. *Int. J. Mass Spectrom.* **2012**, *313*, 30−35.
(79) Echt, O.; Dao, P. D.; Morgan, S.; Castleman, A. W. Multiphoton Ionization of Ammonia Clusters and the Dissociation Dynamics of Protonated Cluster Ions. *J. Chem. Phys.* **1985**, *82*, 4076−4085.

DOI: 10.1021/acs.jpca.9b02768
J. Phys. Chem. A 2019, 123, 4599−4608